



TITLE:

Fast Neutron Fields Produced by Kyoto University Cyclotron (Commemoration Issue Dedicated to Professor Sakae Shimizu on the Occasion of his Retirement)

AUTHOR(S):

Miyajima, Junko; Nishidai, Takehiro; Takekoshi, Hidekuni

CITATION:

Miyajima, Junko ...[et al]. Fast Neutron Fields Produced by Kyoto University Cyclotron (Commemoration Issue Dedicated to Professor Sakae Shimizu on the Occasion of his Retirement). Bulletin of the Institute for Chemical Research, Kyoto University 1979, 57(1): 147-156

ISSUE DATE:

1979-03-31

URL:

<http://hdl.handle.net/2433/76808>

RIGHT:

Fast Neutron Fields Produced by Kyoto University Cyclotron

Junko MIYAJIMA*, Takehiro NISHIDAI**, and Hidekuni TAKEKOSHI*

Received November 16, 1978

Beams of fast neutrons were produced by Kyoto University Cyclotron, using the $^9\text{Be}(d, n)^{10}\text{B}$ reaction.

A number of physical properties of fast neutron fields have been measured for the purpose of radiobiological experiments. These include the effectiveness of neutron collimator, the neutron energy distributions, and the estimation of the neutron component and γ -ray component of absorbed dose in tissue.

KEY WORDS Fast neutron / TOF of fast neutron / Absorbed dose /
Ionization chamber / RBE value of neutron /

I. INTRODUCTION

Intensive radiobiological researches concerning neutron radiotherapy have been endured since new clinical studies were undertaken with Medical Research Council Cyclotron at Hammersmith Hospital in London in 1968. As the results of these studies, significant advantages of neutron beams in therapeutical application are now widely recognized.

Radiobiological advantages of fast neutron beams are shown as follow;

- 1) Fast neutrons have high RBE (relative radiobiological effectiveness) values compared with usually using x-rays, γ -rays or electron beams.
- 2) Recovery of fast neutron irradiated tumorous cells is hindered more than the cases of x-rays, γ -rays or electron beams.
- 3) OER (oxygen enhancement ratio) values of fast neutrons are lower than those of x-rays, γ -rays or electron beams.

As mentioned above, fast neutron beams are expected to damage significantly cells in cancer beyond a cure with x-rays, γ -rays, or electron beams.

Clinical trials of fast neutron beams should be performed under the following conditions.¹⁾

- 1) The 50% depth-dose for a 5 cm by 5 cm irradiation field should occur 10 cm or more below the surface in a unit density tissue equivalent medium.
- 2) The dose rate should exceed 0.1 Gy/min (Gy=joules/kg) on the tumor tissue.
- 3) To satisfy the condition 1) and 2) neutron energy should exceed 14 MeV.

* 宮嶋純子, 竹腰秀邦: Nuclear Science Research Facility, Institute for Chemical Research, Kyoto University, Kyoto.

** 西台武弘: Department of Radiology, Faculty of Medicine, Kyoto University, Kyoto.

The above conditions are currently limited by the availability of suitable neutron sources. There are two reactions are generally known for fast neutron generation. One such reaction is the ${}^3\text{H}(\text{d}, \text{n}){}^4\text{He}$ reaction, in which a beam of deuterons of fairly low energy, such as 200–300 keV, are directed onto a target. In the ensuing reaction, very energetic (14 MeV) neutrons are ejected with approximately uniform flux in all direction. But the output yield with this type reaction is not sufficient for therapy at present. Another useful deuteron induced reaction for producing neutron beams occurs when beam of higher energy deuterons (~ 14 –50 MeV) impinges upon a target of low atomic number, such as beryllium. In this process, the stripping process,²⁾ the deuteron is torn apart in passing through the target material and ejected neutrons peak strongly in a forward direction.³⁾ The mean energy of neutrons, \bar{E}_n in MeV, produced by bombarding thick beryllium target with deuterons of various energies is derived as a function of incident deuteron energy E_d in MeV from the experimental results.⁴⁾

$$\bar{E}_n = 0.43E_d \quad (1)$$

And the dose rate D in wet tissue is expressed as follows,⁵⁾

$$D = 2.7 \times 10^{-6} E_d^{2.7} \quad \text{Gy}/(\mu\text{A} \cdot \text{min}) \quad (2)$$

at a distance of 1.25 m from the source (1.25 m SSD).

At Kyoto University Cyclotron, the average absorbed dose rate should be about 8×10^{-8} Gy/min at 1.25 m SSD from this formula.

However this value is not sufficient for therapy that requires the dose rate more than 0.1 Gy/min, if the SSD 0.5 m is chosen, the absorbed dose 0.05 Gy/min should be achieved and the value should be enough for basic research for the studies of the biological effect of fast neutron. In this paper, we will describe the design parameters to be met in developing facilities for preliminary experiments of clinical trials.

II. FACILITIES

1. Layout of the Cyclotron

The 1.05 m Kyoto University Cyclotron is a fixed energy ordinary cyclotron producing 7.5 MeV protons, 15-MeV deuterons and 30-MeV α s.⁶⁾

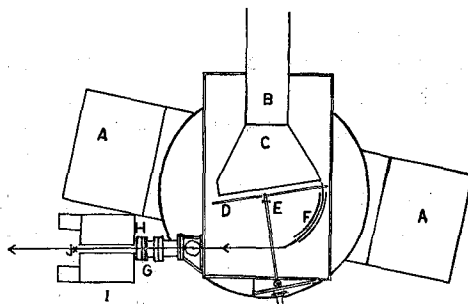


Fig. 1. Layout of the cyclotron and fast neutron treatment area.
A: Magnet, B: Dee stem, C: Dee, D: Dummy dee, E: Ion source,
F: Deflector, G: Target assembly, H: Neutron monitor, I: Collimator,
J: Absorbed dose measurement position (SSD=0.48m).

Figure 1 shows a layout of the cyclotron and fast neutron treatment area. A target assembly is connected with the beam exit of the cyclotron. The deuteron beam current at the radius of final acceleration is 25 μA or less, however, at the exit of the cyclotron it is reduced to 3 μA or less.

2. Target Assembly

Neutrons are produced by deuteron bombardment on water-cooled beryllium target, 2.0 mm thickness. The target assembly is shown in Fig. 2. The target size is a 2.5 cm by 5.0 cm. Deuterons, and the other secondary charged particles are stopped in the beryllium target, in cooling water or in the aluminium backing plate.

3. Neutron Beam Monitoring

The target assembly was electrically isolated from the beam tube and connected to a currentmeter. An ionization chamber was placed behind the target assembly for neutron intensity monitoring. The chamber was a flat cylindrical type and had three 2.0 mm parallel Lucite plates, which were coated with graphite, and two 7.0 mm air gaps. Between the central and side plates in the chamber, 500 V was supplied. The chamber was calibrated nominal to indicate tissue absorbed dose on the beam direction at 0.48 in SSD.

4. Collimation System

We made a beam spot of fast neutrons conform to the tumor size using a collimation system in Fig. 3. Materials constructing the collimation system should be chosen so

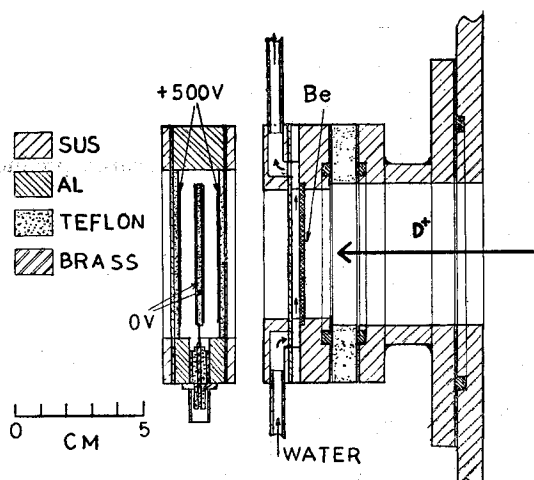


Fig. 2. Cross section of beryllium target assembly and neutron monitoring ionization chamber. The 14-MeV deuteron beam is incident on the thick Be target. A monitoring chamber was located 2.8cm from the target.

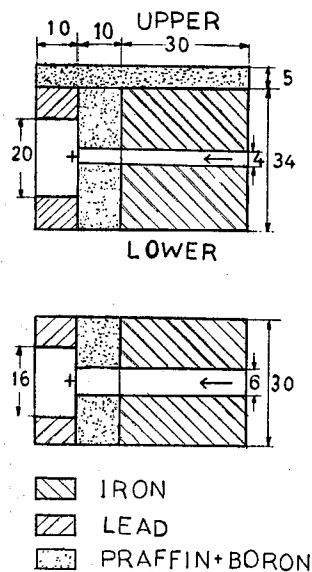


Fig. 3. Cross section of collimator. Beam spot size : 4cm by 6cm, Collimator length : 40cm (30cm of iron, 10cm of paraffin-boron mixture).

as to shield fast neutron effectively. The collimator had an overall length of 40 cm; 30 cm of iron and 10 cm of paraffin-boron mixture. Iron has a large value of macroscopic effective neutron removal cross section,⁷⁾ hydrogen, which is contained fair amount in paraffin, scatters fast neutrons and reduces their kinetic energy effectively, and boron absorbs thermal neutrons. The collimator defined a 4 cm by 6 cm radiation field at the exit. Most measurements using ionization chamber were made in air at 0.48 m SSD. To reduce the neutron and γ -ray background from the adjoining area, the irradiated field was surrounded by blocks of paraffin and lead.

III. MEASUREMENTS

1. Measurements of Collimation

To measure the effectiveness of the collimator, a foil activation method was taken. We employed a $^{27}\text{Al}(n, p)^{27}\text{Mg}$ reaction because of having a suitable threshold energy 2.1 MeV, and also aluminium is easy to deal with.

At the exit of the collimator, segments of aluminium plates, $0.5\text{ cm} \times 1.0\text{ cm} \times 0.2\text{ cm}$, were arranged in a row.

After the irradiation by neutrons, the relative intensities of neutrons were derived from the activation measurements. The results are shown in Fig. 4. A neutron intensity at a shadow 3.5 cm from the edge of the aperture was reduced to 13% from the maximum value. These data show that the fast neutrons exceeding 2.1 MeV were well collimated by the system.

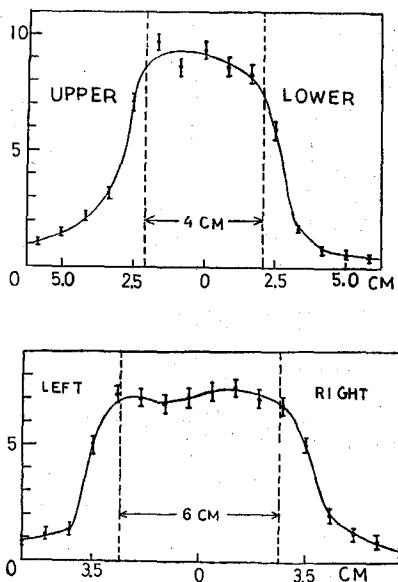


Fig. 4. Relative intensities of fast neutrons at the exit of the collimator by activation method: $^{27}\text{Al}(n, p)^{27}\text{Mg}$

2. Measurements of the Energy Spectra

Neutron energy at 0° were measured using the time-of-flight (TOF) techniques. The experimental setup is shown in Fig. 5. The technique requires short neutron bursts and a detector with fast time response. The neutron bursts were produced by the cyclotron self-bunching beam. The repetition rate was the same as the frequency of the cyclotron rf, 13.05 MHz. A NE 213 organic liquid scintillator, 5.1 cm in diameter by 5.1 cm in length, coupled to a Philips 56DVP photomultiplier tube was used to detect the neutrons at a distance of 1.355 m from the target.

A 23 cm long iron collimator having a 2.4 cm by 2.0 cm aperture was placed in front of the detector, which was housed in the iron and lead shield to reduce room associated background.

The time interval between the bursts was 77 n sec, which was the TOF of 1.6-MeV neutron travelling 1.36 m.

The starting signal was taken from the anode of PM tube. The signal was shaped by a constant-fraction discriminator (ORTEC 271) and a time-pickoff-control (ORTEC 403A), and was supplied to a time-to-amplitude converter (TAC: ORTEC 437A). The stopping signal taken from the cyclotron rf was supplied to the TAC, too, after shaped and delayed. The output signal of the TAC was connected to the input of an analog-to-digital converter (ADC: NS-623). All data-taking was done with an on-line computer (HP 2100).

Dead time of the ADC were kept to less than 13% in all measurements.

Monenergetic neutrons, $E_n = 3.2$ MeV, 4.3 MeV and 5.3 MeV produced by a ${}^7\text{Li}(p, n){}^7\text{Be}$ reaction, were used to determine the relative efficiency of the neutron detector.

The evaluation of the γ -rays contribution and the background neutrons were made by placing lead or beryllium absorber. The neutron energy spectrum shown in Fig. 6 was obtained from the TOF data correcting the detector efficiency and the background evaluations mentioned above.

The present data are in substantial agreement with the other measurements^{8,9,10} and the value derived from the Eq. (1).

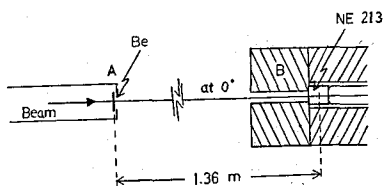


Fig. 5. Schematic illustration of the TOF experimental setup.
Flight path : 1.36m,
A : Target assembly,
B : Iron shield (23cm in length, 2.0 cm by 2.4cm collimation).

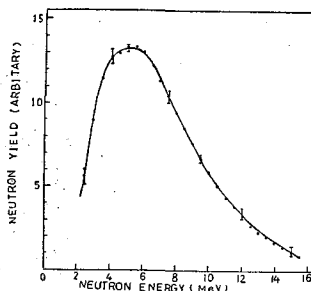


Fig. 6. Neutron spectral distribution from Be+d reaction in thick target.
Target thickness : 2.0mm.

3. Dose Measurements

One of the most general methods for determining absorbed dose should be ionization measurements in gases. Absorbed dose can be estimated using the relation between the ionization produced in a gas-filled cavity at the place of interest in the material irradiated and the energy imparted to unit mass of the material. This is known as the Bragg-Gray relation.¹¹⁾ The dose D in Gy can be written as,

$$D = Q \cdot (W/e) \cdot S/M, \quad (3)$$

where

Q = the ionization in coulombs,

W = the average energy in joules expended by the ionizing particles crossing the cavity,

e = the charge of the electron in coulombs,

S = the effective mass stopping power ratio of medium to that of the cavity gas for those ionizing particles,

M = the mass of the gas in kg.

When dose measurements were made by the ionization chamber method, the operating conditions of a chamber should be arranged to give less than 1% loss of charge by recombination, if possible.

Recombination is usually classified as the term of general or initial recombination.

General recombination increases with radiation intensity, which is the dose rate usually in dosimetry. Whereas, initial recombination is independent of the dose rate. The amount of initial recombination depends upon the LET of the ionizing particle and the strength of collecting field.

As long as the chamber is used to measure the dose of low LET radiation such as x-ray or γ -ray, initial recombination will not affect the measurements. Therefore, the criterion that the loss of ions by general recombination can be neglected should be determined by γ -ray calibration of known dose rate.

The measurements of absorbed dose were performed with two cylindrical ionization chambers shown in Fig. 7. The upper limit to the dose rate of the each chamber was checked by irradiation in the Cs-137 standard field of values from 1.8R/min to 29.9R/min of exposure dose. The each upper limit was 17R/min when the chambers were

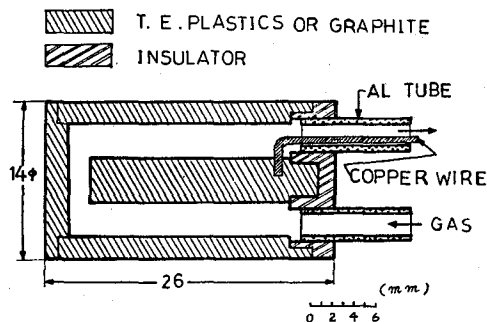


Fig. 7 Cross section of ionization chamber, TEP-TEG and C-air chambers.

supplied more than 200 V. As the maximum observed dose rate 0.1 Gy/min at 0.48 m SSD obtained with the cyclotron was nearly half of 17 R/min, which corresponds to 0.18 Gy/min, the correction of general recombination effect should be neglected.

Significant initial recombination may occur when the ionization by high LET particles is measured with the chamber. As the case, good plateau cannot be observed in saturation measurements, field strength vs. current curve measurements.

Generally, initial recombination is shown in the following relation,¹²⁾

$$1/i = 1/i_{\text{sat}} + \text{constant}/x, \quad (4)$$

where, i is observed ionization current, i_{sat} is true saturation current, x is an appropriate function of the collecting field strength. If the reciprocal of the measured current, $1/i$, is plotted against $1/x$ a straight line will be obtained and a correction factor will be estimated. To determine the value of i_{sat} , the chamber current was measured varying the supplied voltage from 0 V to 1000 V under the dose rate which could neglect the general recombination. The difference between the actually i_{sat} and i was less than 0.1%. This value lies within the overall uncertainty of measurements with the ionization chamber.

One of the ionization chambers was constructed of tissue equivalent (TE) plastic (C: 78.9 wt%, H: 10.1 wt%, O: 4.8 wt%, N: 3.5 wt%, Ca: 1.8 wt%, and F: 1.7 wt%)¹³⁾ and was filled with TE gas (64.4% CH₄, 32.4% CO₂, and 3.2% N₂). It had a nominal cavity volume of 1.3 cm³ with a wall thickness of 2.0 mm. Another chamber had a dimension approximately equal to that of the TE chamber, but was constructed of carbon and filled with air. A cross section of the ionization chambers is shown in Fig. 7.

The TE chamber was used to determine the total absorbed dose in tissue, and the carbon-air (C-air) chamber was used to evaluate the relative component of γ -rays to total absorbed dose.

The response of these chambers, Q_i (in coulombs), in a mixed n - γ field is given by,¹⁴⁾

$$Q_i = A_i D_\gamma + B_i D_n, \quad (5)$$

where D_γ and D_n are the γ and n tissue dose in Gy respectively, and A_i (i means TE chamber or C-air chamber) and B_i are the absorbed dose conversion coefficients in coulombs/Gy for γ -rays and neutrons, respectively.

The values of the γ -ray sensitivity A_i were readily determined to be 4.70×10^{-8} coulombs/Gy $\pm 2.4\%$ for the TE chamber and 5.27×10^{-8} coulombs/Gy $\pm 2.4\%$ for the C-air chamber, by measuring the Cs-137 γ -ray fields.

The Eq. (5) is divided by A_i for calculational convenience and written as

$$(Q_i/A_i) = D_\gamma + (B/A)_i D_n \quad (6)$$

where B_i/A_i is defined as $(B/A)_i$.

The values of B_i , the neutron sensitivity for TE chamber or C-air chamber, were calculated from $(B/A)_i$ using the Bragg-Gray relation, respectively. That is,

$$(B/A)_{\text{TE}} \cong (w_{\text{TEG},\gamma} \times S_{\text{TEG},\gamma}^{\text{TEP}}) / (w_{\text{TEG},n} \times S_{\text{TEG},n}^{\text{TEP}}), \quad (7)$$

$$(B/A)_{C-air} \cong (w_{air,r} \times S_{air,r}^C \times K_T^C) / (w_{air,n} \times S_{air,n}^C \times F_T^C), \quad (8)$$

where,

$w = W/e$, W and e are same one appeared in the Eq. (3),

S = the effective mass stopping power ratio of the chamber wall material (TEP or carbon) to the gas (TEG or air) for γ -rays or neutrons, respectively,

K = the ratio of kerma of carbon to that of tissue for fast neutrons,

F = the ratio of the mass energy-absorption coefficient of carbon to that of tissue for the Cs-137 γ -radiation.

Values of $w_{TEG,r} = 29.2$ joules/coulomb,¹⁵⁾ $w_{TEG,n} = 30.5$ joules/coulomb,¹⁵⁾ $S_{TEG,r}^{TEP} \approx 1^{15)}$ and $S_{TEG,n}^{TEP} \approx 1^{15)}$ were used in a homogeneous chamber in the calculation for the Eq. (7). As the result, the ratio $(B/A)_{TE}$ was determined to be 0.96. In the Eq. (8), values of $w_{air,r} = 33.7$ joules/coulomb,¹⁵⁾ $w_{air,n} = 34.9$ joules/coulomb,¹⁶⁾ $S_{air,r}^C = 1.01$,¹⁴⁾ $S_{air,n}^C \cong S_{air,p}^C = 1.04$ ¹⁶⁾ and $F_T^C = 0.906$ ¹⁴⁾ were used. The ratio of kerma $K_T^C = 0.116$ was obtained by weighted-averaging over the measured neutron energy spectrum in Fig. 6 using the kerma value for each neutron energy calculated by Caswell *et al.*^{18,19)}

The value of $(B/A)_{C-air}$ was calculated to be 0.12.

It becomes possible to separate the absorbed dose due to neutrons and that of γ -rays by using the values of A_i , B_i .

In the measurements of the absorbed dose in air, the chamber wall should be thick enough that most of the secondary particles produced in air can not reach the cavity of the chamber. But the chamber wall absorbs and scatters the primary radiation, so it is undesirable to make the wall any thicker than is necessary. It implies the satisfaction for the charged particle equilibrium (CPE) condition^{14,20)} in the cavity and its immediate surroundings.

From the consideration of the CPE criterion, it should be optimum for a wall thickness to be equal to the maximum range of the most energetic secondary particles. The most energetic protons generated in TE plastic by 9 MeV neutrons have a range of 1.1 mm.²¹⁾ The neutrons higher than 9 MeV was less than 30% in measured neutron energy spectrum. The secondary particles generated in carbon by neutrons are mainly α -particles and even the most energetic secondary has a shorter range than the secondary protons produced by 9 MeV neutrons. So, the actual wall thickness should be enough to be CPE with neutrons. However, a wall thickness 2.0 mm is somewhat thinner than the maximum range of the secondary electrons of the Cs-137 γ -rays, that is 4.5 mm.¹⁴⁾ Put a 2.5 mm thick cap on the chamber, the resultant wall thickness is 4.5 mm and the CPE condition for the Cs-137 γ -rays will be satisfied. Whether the difference between the two cases would be able to observe or not was examined by current measurements in the Cs-137 γ -field. The difference being due to thickness were estimated less than 2.4% for measured currents in both TE and C-air chambers.

Thus, the absorbed doses due to neutrons and γ -rays were obtained in the n- γ mixed field produced by the cyclotron. The ratio of the γ -ray component to the neutron component, D_γ/D_n , is 0.3 ± 0.02 in tissue absorbed dose measurements at 0.48 m SSD. The averaged dose rate was about 0.06 Gy/min at that point.

4. Biological Characteristics of the Neutron Beam

As the preliminary clinical trials, the RBE values of fast neutron beams produced by the cyclotron were measured by a group of Professor Abe of Kyoto University Hospital. The outline of the results is presented in the following.²²⁾

Relative effectiveness of fast neutron beams vs Co-60 γ -rays, Cs-137 γ -rays and 32 MeV electron beams were derived from the each dose response curve on the growth delay-time for C3H/He mouse mammary carcinoma.

The values were reduced continuously from 5.0 to 3.0 as compared with Cs-137 γ rays (0.15 Gy/min) and from 4.2 to 2.7 as compared with 32-MeV electron beams (15 Gy/min). However, the values as compared with Co-60 γ rays (1.5 Gy/min) were smaller than those compared with 32-MeV electron beams on 1 to 6 growth delay-days, and were similar to those for Cs-137 γ rays on 8 to 20 growth delay-days.

The results are shown in Figs. 8 and 9.

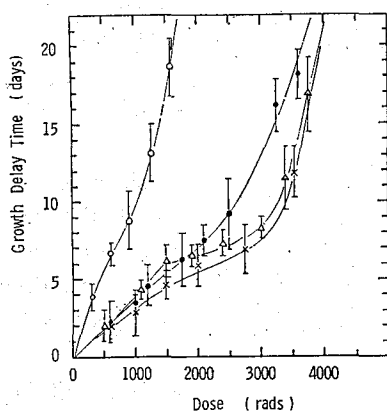


Fig. 8. Dose response curves on growth delay-time for C3H/He mouse mammary carcinoma, irradiated with n- γ mixed beams (0.08 Gy/min, ○), 32-MeV electron beams (15 Gy/min, ●), ^{60}Co γ rays (1.5 Gy/min, △) and ^{137}Cs γ rays (0.15 Gy/min, ×)

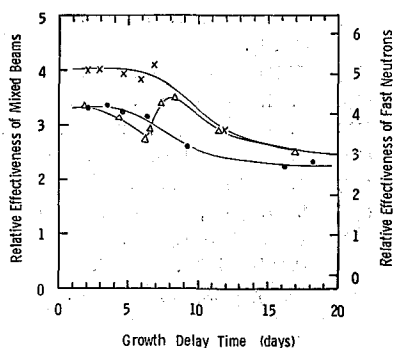


Fig. 9. Relative effectiveness of n- γ mixed beams or fast neutrons alone (0.05-0.06 Gy/min), compared with 32-MeV electron beams (●), ^{60}Co γ rays (△), ^{137}Cs γ rays (×) irradiations.

ACKNOWLEDGMENTS

The authors wish to thank Dr. T. Hiraoka of National Institute of Radiological Sciences, Chiba, for his advice on design of the TE chamber and for supplying them with TE plastics. They are also indebted to professors M. Abe and T. Yanabu for drawing for their attention to this problem and wish to thank to staffs of the Kyoto University Cyclotron for their helps. This paper is dedicated to professor S. Shimizu on the commemoration of his retirement.

REFERENCES

- (1) P. Wooton, K. Alvar, H. Bichsel, J. Eenmaa, J. S. R. Nelson, R. G. Parker, K. A. Weaver, D. L. Willams, and W. G. Wyckoff *J. Canadian Associat. Radiol.*, **26**, 44 (1975).
- (2) R. Serber, *Phys. Rev.*, **73**, 1008 (1947).
- (3) L. S. August, F. H. Attix, G. H. Herling, P. Shapiro, and R. B. Theus, *Phys. Med. Biol.*, **21**, 931 (1976).
- (4) C. J. Parnell, G. D. Almond, and J. B. Smathers, *Phys. Med. Biol.*, **17**, 429 (1972).
- (5) K. Kawashima, *Jap. J. Cancer Clinics*, **23**, 268 (1977).
- (6) Y. Uemura, K. Fukunaga, S. Kakigi, T. Yanabu, N. Fujiwara, T. Ohsawa, H. Fujita, T. Miyanaga, and D. C. Nguyen, *Bull. Inst. Chem. Res., Kyoto Univ.*, **51**, 87 (1974).
- (7) S. G. Tsypin, *Atomnaya Energiya*, **12**, 300 (1962).
- (8) M. A. Lone, Symposium on Neutron Cross Sections from 10 to 40 Mev held at BNL, May 3-5, 1977, BNL-NCS-50681, 79 (1977).
- (9) M. A. Lone, C. B. Bigham, J. S. Fraser, H. R. Schneider, T. K. Alexander, A. J. Ferguson, and A. B. McDonald, *Nucl. Instr. & Meth.*, **143**, 331 (1977).
- (10) M. J. Saltmarsh, C. A. Ludemann, C. B. Fulmer, and R. C. Styles, *Nucl. Instr. & Meth.*, **145**, 81 (1977).
- (11) T. E. Burlin, Radiation Dosimetry, vol. I, (Academic Press) 332-392 (1966).
- (12) P. B. Scott and J. R. Greening, *Phys. Med. Biol.*, **8**, 51 (1963).
- (13) T. Hiraoka, K. Kawashima, K. Hoshino, and H. Matsuzawa, *Nippon Acta Radiol.*, **25**, 420 (1976).
- (14) ICRU Report 10b, NBS Handbook 85, (1962).
- (15) A. R. Smith, *Med. Phys.*, **2**, 195 (1975).
- (16) H. Bichsel, Univ. of Washington Internal Report #77.5 (1977).
- (17) R. L. Caswell and J. J. Coyne, *Radiat. Res.*, **52**, 448 (1972).
- (18) R. L. Bach and R. S. Caswell, *Radiat. Res.*, **35**, 1 (1968).
- (19) J. W. Boag, Radiation Dosimetry, vol. II, (Academic Press) (1966).
- (20) C. F. Williamson, J. P. Boujet, and J. Picard, Report CEA-R3042 (Saclay).
- (21) T. Nisidai, M. Abe, Y. Yukawa, S. Suyama, J. Miyajima, and H. Takekoshi, *J. Jap. Soc. Cancer Ther.*, **14**, 1 (1979).